



## Shear Behavior of Pre-Cracked RC Plates Subjected to Combined Axial and Shear Stress

Yoshio Kitada<sup>1)</sup>, Takao Nishikawa<sup>2)</sup>, Koichi Maekawa<sup>3)</sup>, Katsuhiko Umeki<sup>4)</sup>,  
Mamoru Yamada<sup>4)</sup> and Kazunori Kamimura<sup>4)</sup>

1) Nuclear Power Engineering Corporation, Japan

2) Tokyo Metropolitan University, Japan

3) The University of Tokyo, Japan

4) Obayashi Corporation, Japan

**ABSTRACT :** The paper describes the summary of the test performed to develop a new constitutive law of shear transfer in a reinforced concrete (RC) seismic shear wall through tensile cracks. The test was performed for 12 RC plate specimens by loading shear force under a constant axial stress condition. The paper presents the outline of specimen, the loading test-setup and test data measurement. Also, results of the test data of the 12 specimens, the influence of axial stress and reinforcing ratio on shear transfer mechanism through tensile concrete cracks at RC plates are addressed.

### 1. INTRODUCTION

In the current seismic design of nuclear power plant (NPP) buildings in Japan, seismic design loads in the two orthogonal horizontal directions are determined independently by seismic response analyses, whereas actual earthquake motion strikes the buildings in all three directions simultaneously. In order to clarify the effect of multi-directional input forces to RC (seismic) shear wall, which is a main earthquake-resistance element in NPP buildings, Nuclear Power Engineering Corporation (NUPEC) has been conducting a project of "Model Tests of Multi-Axis Loading on RC Shear Walls". The major objective of the project is to accumulate static and dynamic test data of multi-directional simultaneous loading tests of RC shear walls.

A seismic shear wall in a building is loaded inevitably by both axial and shears forces repeatedly during an earthquake. Under the situation, horizontal tensile cracks are generated due to the axial force at the flange portion, and shear cracks are generated due to the shear force at the web portion. The prediction of nonlinear behavior of the shear wall with those cracks, especially the shear transfer mechanism through cracks is very important in the building seismic design. Nevertheless, the studies related to this point of view have been limited in number. The main purpose of the present study is to develop a new constitutive law of shear transfer in a RC seismic shear wall through existing cracks.

### 2. TEST SPECIMEN

#### 2.1 Test Parameter

Test Parameter, i.e., reinforcing ratio ( $P_s$ ) and axial stress level ( $\sigma_o$ ), are listed in Table 1 for 12 test specimens. Those were determined based on the survey of actual reactor building design conditions. The difference of the reinforcing ratios are achieved by using rebars of different diameter (D) as 13, 16 and 22 in millimeters and described as D13, D16 and D22. The axial stress applied is given as a test parameter ranging from 3.0MPa in compression to

3.0Mpa in tension.

### *2.2 Dimensions of Test Specimen*

The test specimens are square reinforced concrete plates having dimension of 1.2m×1.2m×0.2m as shown in Fig. 1. In order to apply axial and shear stress to the specimen, several loading bolts are placed on four sides of the specimens. And, steel plates are padded at the outer portion of the specimen, in order to prevent a local concrete failure.

### *2.3 Reber Arrangement*

Rebar arrangement of the specimens is shown in Fig.2. Main rebars are double and arranged orthogonally in a pitch of 150mm, and the shear rebars (D6) are arranged at the center of the specimen so that the reinforcing ratio becomes the same as that of actual building. Near the side of the specimen, shear rebars are arranged to prevent a local concrete failure.

### *2.4 Material Properties*

The design strength of the concrete is 30Mpa, and the rebar-yielding stress is 345Mpa. The material properties of concrete and rebars obtained by material test are listed in Table 2. The notation of specimen such as D13+1.5 is determined in the manner that diameter of reinforcing bar of 13mm and applied axial compression stress of 1.5MPa.

## 3. LOADING PLAN

### *3.1 Loading Test Setup*

The loading test setup is shown in Fig.3 (a), (b) and photo 1. The loading test setup consists of reaction frame, loading bars made of high strength steel and loading jacks. Tension force is applied by four 1000kN jacks, placed outside of the reaction frame, and compression force is applied by four 1000kN jacks, placed inside of the reaction frame. The shear force is applied by four 5000kN jacks through high strength steel bars.

### *3.2 Loading Program*

Loading program is shown in Fig.4 (a) and (b). At first, specimen is tensioned up to 3Mpa in order to generate horizontal tensile cracks. Secondly, the specified axial stress shown in Table 3 is applied. Then thirdly, holding the axial stress constant, the cyclic shear stress is applied repeatedly with increasing the load up to failure. The applied load control is performed firstly by the load-control increasing load by 0.25-0.5Mpa until the generation of shear cracks, then it is changed by the displacement-control increasing shear strain by 1000  $\mu$ .

## 4. MEASUREMENT

Measurement in the test was carried out on axial and shear stresses, axial displacements, shear strains and rebar strains. Fig.5 shows the arrangement of displacement transducers. Cracks and crack patterns are checked by visual inspection and marked as a record. Axial and shear stresses are measured by the load cells attached on the loading jacks. Furthermore, axial displacements and shear strains are measured by the displacement transducers attached on the both sides at the center of the specimen. The rebar strains are measured by the foil strain gauges attached on the both sides of rebars.

## 5. TEST RESULTS AND INVESTIGATION

### *5.1 Stress-Strain Relationship*

Typical tensile stress-strain ( $\sigma - \epsilon$ ) relationship is shown in Fig.6(a) for the specimen of D22+1.5. Also shear stress-strain ( $\tau - \gamma$ ) relationship of specimens, D13+1.5, D16+3.0 and D22+1.5 are shown in Fig. 6(b), 6(c) and 6(d) respectively as typical examples. The shear

stresses at shear cracking ( $\tau_c$ ), rebar yielding ( $\tau_y$ ) and ultimate ( $\tau_u$ ) are shown in those figures using symbols ●, ○, ▼ respectively. Furthermore, the calculated shear stresses at rebar yielding ( $\tau_y(\text{cal})$ ), and ultimate rebar strength ( $\tau_u(\text{cal})$ ) are added on Fig.6. Those stresses are calculated by the following equations;

$$\tau_y(\text{cal}) = \sqrt{P_s \cdot s_{\sigma y} (P_s \cdot s_{\sigma y} - \sigma_0)} \quad \dots (1),$$

$$\tau_u(\text{cal}) = \sqrt{P_s \cdot s_{\sigma B} (P_s \cdot s_{\sigma B} - \sigma_0)} \quad \dots (2),$$

where,  $s_{\sigma y}$ : Rebar Yield Stress,  $s_{\sigma B}$ : Rebar tensile Strength,  $\sigma_0$ : Axial stress,  $P_s$ : Reinforcing Ratio.

In Fig.6,  $\tau_u$  values agree well with the  $\tau_u(\text{cal})$  values obtained using Eq.(2) in the test series of D13, because these values are strongly influenced by rebar strength. On the other hand, the  $\tau_u$  values are much smaller than the  $\tau_u(\text{cal})$  values in the test series of D22 because those are strongly influenced by concrete failure.

### 5.2 Crack patterns

Crack patterns of the specimen(D13+1.5) are shown in Fig.7(a)~(d) as a typical example. Initial horizontal cracks and shear cracks are distributed to the whole specimen, and the proper stress distribution can be confirmed from these crack patterns.

### 5.3 Test Results

#### (1) measurement values

Major measurement results are listed in Table 4. The axial stress and shear stresses at initial horizontal crack generation, ( $n\sigma_c$ ) and  $\tau_c$ , are determined based on visual inspection of the axial cracks. The values of  $\tau_y$  means the shear stress at which rebar is yield. The value is determined based on the material test results. The values of  $\tau_u$ , the maximum value of  $\tau$ , are obtained from the  $\tau - \gamma$  relationship. Furthermore, initial shear modulus,  $G_i$ , is obtained based on the least square fitting results applied to  $\tau - \gamma$  envelope curve between the values, 0 and  $\tau_c$ .

#### (2) Normalization of Measured Values

In order to eliminate the effect of the differences in material strength, the values of  $\tau_c$  are normalized by the concrete tensile strength,  $cft$ , and the values of  $\tau_y$  and  $\tau_u$  are normalized by the value of  $P_s \cdot s_{\sigma y}$  respectively to have  $\tau_c/cft$ ,  $\tau_y/P_s \cdot s_{\sigma y}$ ,  $\tau_u/P_s \cdot s_{\sigma y}$ . Furthermore,  $G_i$  is also normalized by the elastic shear modulus,  $G_0$ , to have shear modulus reduction factor,  $G_i/G_0$ , caused by cracking.

#### (3) Influence of axial stress level and reinforcing ratio

The relationships between  $\tau_c/cft$  and axial stress are shown in Fig.8(a). The  $\tau_c/cft$  value is changing depending on the axial stress applied and is larger for axial tension load than for axial compression load. Though the relationship between D13 and D16 in the compression side is reverse of those of tension side, the influence of this phenomenon on  $G_i/G_0$  is small from calculation study results. The influence of reinforcing ratio on  $\tau_c/cft$  is not so large.

The relationships between  $G_i/G_0$  and axial stress are shown in Fig.8(b). The maximum value is obtained as 84% for D13-1.5 specimen and minimum value is obtained as 17% for D16+3.0 specimen. The overall tendency in the figure shows that the  $G_i/G_0$  value is strongly depend on the axial stress value having larger value for axial tension load than for axial compression load and the influence of reinforcing ratio on  $G_i/G_0$  is small.

## 6. CONCLUSIONS

Combined axial and shear loading test of 12 RC plates has been performed to develop a new constitutive law of shear transfer in RC through tensile cracks. Followings are major test results.

- (1) The failure of the specimens of D13 and D16 series began with concrete shear crack, then rebar yielded and finally concrete crush occurred.
- (2) The failures of the D22 series specimens were different from those of D13 and D16 series, because concrete crush occurred prior to the rebar yielding.
- (3) The maximum value of shear modulus reduction factor ( $G_i/G_0$ ) is 84% for the case of D13-1.5 specimen and the minimum value is 17% for the case of D16+3.0 specimen respectively. The factors varied depending on the axial stress applied.
- (4) The shear modulus reduction of RC shear walls after having tensile crack varies large depending on the applied load etc. Thus a proper constitution law for RC shear walls having tensile cracks is needed to comprehend their nonlinear behavior under multi-axis loading condition.

## 7. ACKNOWLEDGMENTS

This study has been conducted by NUPEC as a project commissioned by the Ministry of International Trade and Industry (MITI) of Japan. The whole study has been steering by the committee of this project. The authors wish to express their gratitude to all members of the committee for their encouragement and valuable discussions given in technical meetings.

## REFERENCES

- 1) Habasaki, A. et al., : Multi-axial Loading Test for RC Wall of Reactor Building, submitted to 15th SMiRT, 1999.
- 2) Yamada, K. and Aoyagi, Y., : Shear Transfer Across Crack, Proceedings of JCI 2nd Colloquium on shear analysis of RC structures, pp.19-28, Oct., 1983.
- 3) Al-Mahaidi, R. S. H. : Nonlinear Finite Element Analysis of Reinforced Concrete Deep Members, Report 79-1, Department of Structural Engineering, Cornell University, 1979.
- 4) Naganuma, K. : Nonlinear Analytical Model for Reinforced Concrete Panels under In-plane Stresses, Study on Nonlinear Analytical method for reinforced concrete wall structure (Part 1), Journal of Struct. Constr. Engng., AIJ, No.421, Mar., 1991.

Table 1 Test Specimen and Parameter

| $\sigma_0$<br>Axial<br>Stress (MPa) \ $P_s$ (%) | 0.84<br>[D13] | 1.32<br>[D16] | 2.58<br>[D22] |
|---|---------------|---------------|---------------|
| -2.94[-3.0]                                     |               | ○             |               |
| -1.47[-1.5]                                     | ○             | ○             | ○             |
| 0.0 [0.0]                                       | ○             | ○             | ○             |
| +0.73 [0.75]                                    |               | ○             |               |
| +1.47 [1.5]                                     | ○             | ○             | ○             |
| +2.94 [3.0]                                     |               | ○             |               |

[ ] : Name of Test Specimen

- : Axial Compression

+ : Axial Tension

Table 2 Material Properties

| Specimen Name | Concrete                  |                                     |  |                                   |                       |
|---------------|---------------------------|-------------------------------------|--|-----------------------------------|-----------------------|
|               | Age (Day)                 | Compressive Strength $\sigma$ (MPa) | Strain at Max. Stress $\epsilon$ ( $\mu$ ) | Young's Modulus $E$ (GPa)         | Poisson's Ratio $\nu$ |
| D13+1.5       | 182                       | 22.8                                | 2414                                       | 21.0                              | 0.185                 |
| D13±0.0       | 224                       | 25.2                                | 1969                                       | 21.8                              | 0.171                 |
| D13-1.5       | 210                       | 24.0                                | 1988                                       | 21.2                              | 0.201                 |
| D16+3.0       | 234                       | 23.7                                | 2182                                       | 21.9                              | 0.172                 |
| D16+1.5       | 275                       | 26.7                                | 2116                                       | 25.1                              | 0.189                 |
| D16+0.75      | 289                       | 26.6                                | 2130                                       | 23.2                              | 0.166                 |
| D16±0.0       | 303                       | 26.3                                | 2094                                       | 22.7                              | 0.189                 |
| D16-1.5       | 344                       | 30.2                                | 2307                                       | 24.8                              | 0.165                 |
| D16-3.0       | 315                       | 26.7                                | 2128                                       | 24.2                              | 0.166                 |
| D22+1.5       | 35                        | 31.8                                | 2668                                       | 26.7                              | 0.189                 |
| D22±0.0       | 28                        | 30.8                                | 2408                                       | 26.8                              | 0.165                 |
| D22-1.5       | 49                        | 32.5                                | 2128                                       | 26.6                              | 0.166                 |
| Rebar         |                           |                                     |  |                                   |                       |
| Rebar         | Young's Modulus $E$ (GPa) | Elongation $P_w$ (%)                | Yield Strength $s \sigma$ (MPa)            | Tensile Strength $s \sigma$ (MPa) |                       |
| D13           | 193.2                     | 0.84                                | 354.7                                      | 537.9                             |                       |
| D16           | 193.2                     | 1.32                                | 372.8                                      | 581.1                             |                       |
| D22           | 193.7                     | 2.58                                | 373.7                                      | 572.7                             |                       |

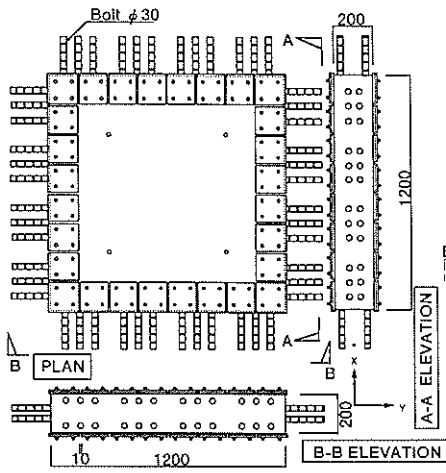


Figure 1 Configuration and Size of Test Specimen

**Strain Gages**

- Both Sides of X-Direction Main Rebar(24)
- Both Sides of Y-Direction Main Rebar(24)
- ◇ Center of Additional Rebar(4)
- Both Sides of Diagonal Steel Bar(16)

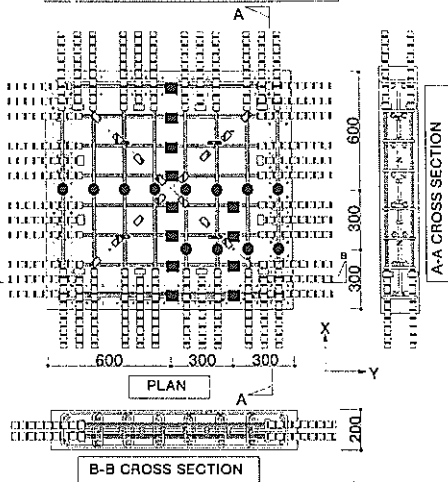


Figure 2 Rebar Arrangement of Test Specimen

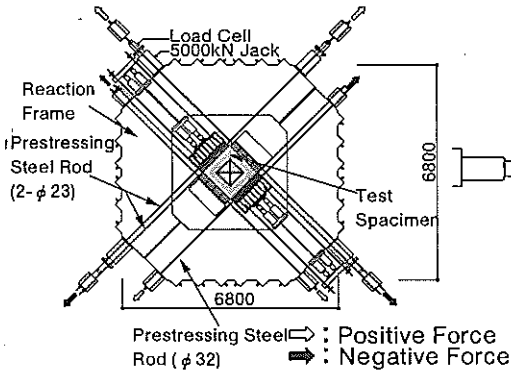


Figure 3(a) Loading Setup (Plan)

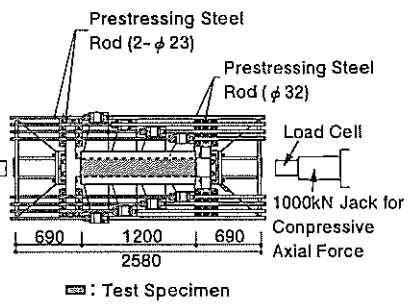


Figure 3(b) Loading Setup (Elevation)

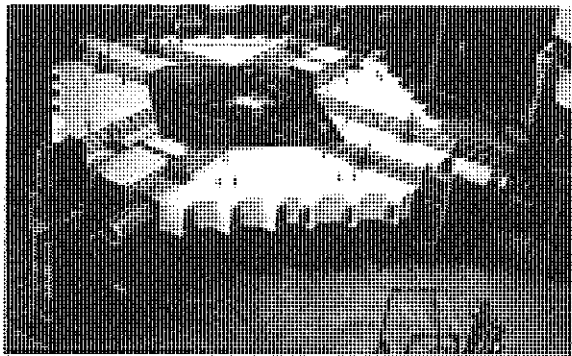


Photo 1 Loading Setup and Test Specimen

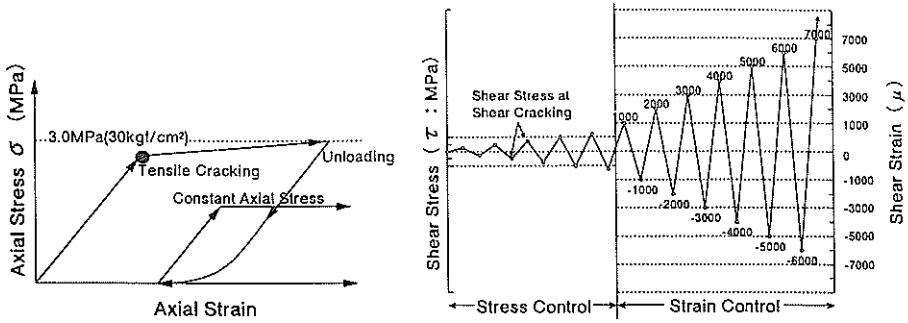


Figure.4(a) Loading Pattern (Axial Stress) Figure.4(b) Loading Pattern (Shear Stress)

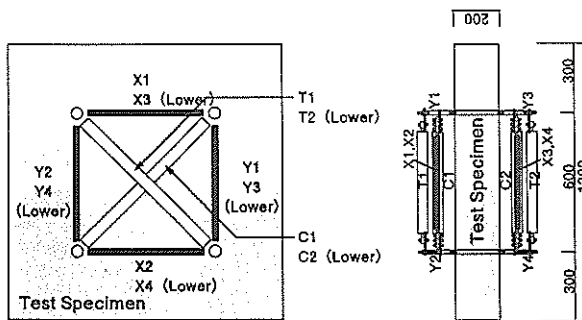


Figure 5 Transducer Arrangement

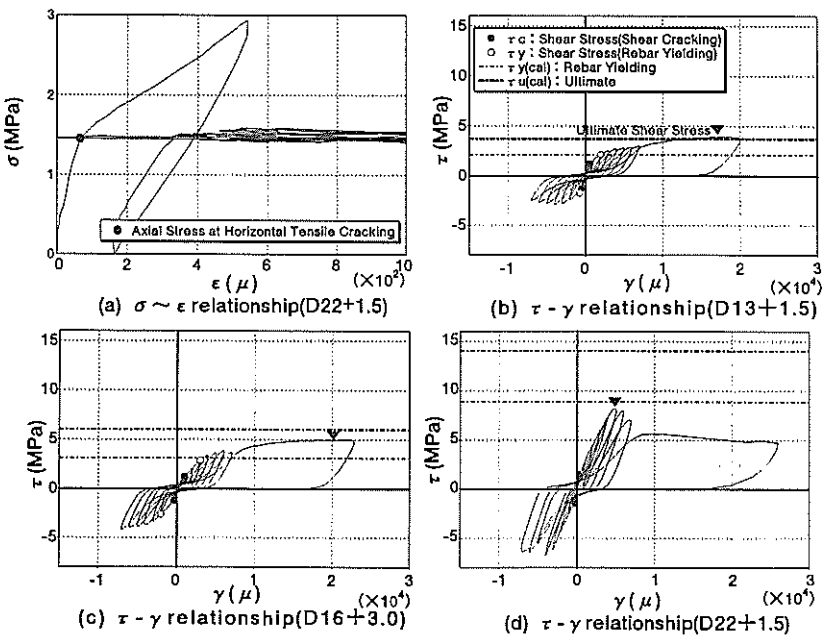


Figure 6 Representative  $\sigma \sim \epsilon$ ,  $\tau \sim \gamma$  Relationship

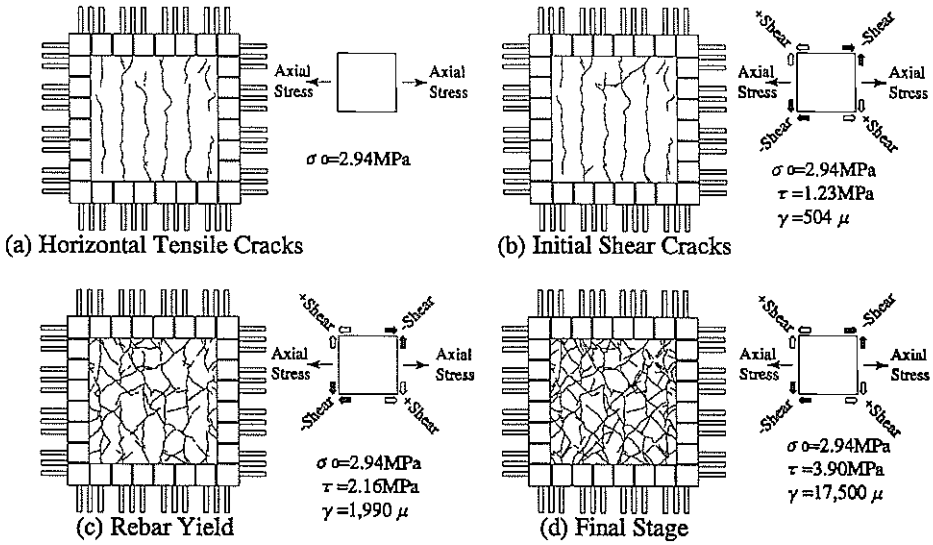


Figure 7 Crack Pattern(D13 + 1.5)

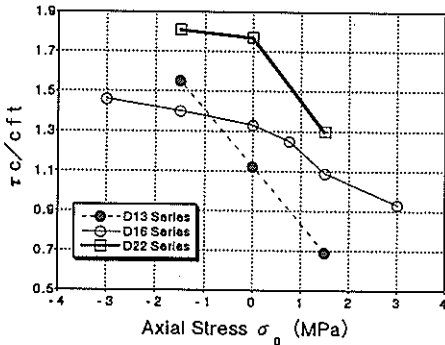


Figure 8(a) Shear Stress at Shear Cracking - Axial Stress

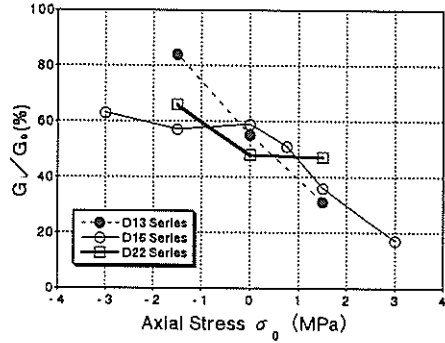


Figure 8(b) Shear Modulus Reduction Factor - Axial Stress

Table 3 Test Results

| Specimen Name | Horizontal Tensile Crack        |                                     | Shear Crack                  |                                  | Rebar Yield                       |                                       | Ultimate Shear Stress             |                                       | Initial Stage Shear Stiffness |             | Concrete Elastic Shear Modulus |                 | Shear modulus reduction factor |  |
|---------------|---------------------------------|-------------------------------------|------------------------------|----------------------------------|-----------------------------------|---------------------------------------|-----------------------------------|---------------------------------------|-------------------------------|-------------|--------------------------------|-----------------|--------------------------------|--|
|               | $\frac{n\sigma_c}{c f_t}$ (MPa) | $\frac{n\sigma_c}{c f_t}$ ( $\mu$ ) | $\frac{\tau_c}{c f_t}$ (MPa) | $\frac{\tau_c}{c f_t}$ ( $\mu$ ) | $\frac{\tau_y}{P_{s-y}G_s}$ (MPa) | $\frac{\tau_y}{P_{s-y}G_s}$ ( $\mu$ ) | $\frac{\tau_u}{P_{s-u}G_s}$ (MPa) | $\frac{\tau_u}{P_{s-u}G_s}$ ( $\mu$ ) | $G_i$ (GPa)                   | $G_0$ (GPa) | $G_i/G_0$                      | $G_i/G_0$ (ksi) |                                |  |
| D13+1.5       | 1.87                            | 1.77                                | 1.23                         | 0.69                             | 2.16                              | 0.72                                  | 3.90                              | 1.31                                  | 17500                         | 8.86        | 31                             |                 |                                |  |
| D13±0.0       | 1.67                            | 1.54                                | 1.72                         | 1.12                             | 3.12                              | 1.05                                  | 4.53                              | 1.52                                  | 23400                         | 9.31        | 55                             |                 |                                |  |
| D13-1.5       | 1.33                            | 1.26                                | 1.95                         | 1.55                             | 4.16                              | 1.39                                  | 5.08                              | 1.70                                  | 20000                         | 9.04        | 84                             |                 |                                |  |
| D16+3.0       | 1.61                            | 1.33                                | 1.24                         | 0.93                             | 2.88                              | 0.59                                  | 4.94                              | 1.00                                  | 20000                         | 9.34        | 17                             |                 |                                |  |
| D16+1.5       | 1.48                            | 1.14                                | 1.24                         | 1.09                             | 4.47                              | 0.91                                  | 6.08                              | 1.24                                  | 20100                         | 10.56       | 36                             |                 |                                |  |
| D16+0.75      | 1.29                            | 1.16                                | 1.45                         | 1.25                             | 4.72                              | 0.96                                  | 6.34                              | 1.29                                  | 18100                         | 9.93        | 51                             |                 |                                |  |
| D16±0.0       | 1.39                            | 1.19                                | 1.58                         | 1.33                             | 5.11                              | 1.04                                  | 6.49                              | 1.32                                  | 14500                         | 9.55        | 59                             |                 |                                |  |
| D16-1.5       | 1.53                            | 1.41                                | 1.98                         | 1.40                             | 5.47                              | 1.11                                  | 7.31                              | 1.48                                  | 13100                         | 10.64       | 57                             |                 |                                |  |
| D16-3.0       | 1.41                            | 1.32                                | 1.93                         | 1.46                             | 6.20                              | 1.26                                  | 7.52                              | 1.52                                  | 11000                         | 10.38       | 63                             |                 |                                |  |
| D22+1.5       | 1.46                            | 1.14                                | 1.48                         | 1.30                             | —                                 | —                                     | 8.16                              | 0.85                                  | 5030                          | 11.23       | 47                             |                 |                                |  |
| D22±0.0       | 1.47                            | 1.15                                | 2.03                         | 1.77                             | —                                 | —                                     | 8.74                              | 0.91                                  | 4830                          | 11.50       | 48                             |                 |                                |  |
| D22-1.5       | 1.66                            | 1.21                                | 2.19                         | 1.81                             | —                                 | —                                     | 9.34                              | 0.97                                  | 5010                          | 11.41       | 66                             |                 |                                |  |

$n^{\sigma} c$ : Axial Stress at Horizontal Cracking  
 $n^{\epsilon} c$ : Axial Strength at Horizontal Cracking  
 $\tau_c$ : Shear Stress at Shear Cracking  
 $\gamma c$ : Shear Strength at Shear Crack Occurring  
 $cft$ : Tensile Strength of Specimen Concrete  
 $G_0 = cE/2(1 + \nu)$ ,  $cE$ : Concrete Young's Modulus  
 $\tau_y$ : Shear Stress at Rebar Yielding  
 $\gamma_y$ : Shear Strain at Rebar Yielding  
 $\tau_u$ : Ultimate Shear Stress  
 $\gamma_u$ : Ultimate Shear Strain at  $\tau_u$   
 $G_i$ : Initial Stage Shear Stiffness  
 $\sigma_B$ : Compressive Strength of Concrete  
 $P_s$ : Reinforcing Ratio  
 $s^{\sigma} \gamma$ : Rebar Yield Stress  
 $\nu$ : Concrete Poisson's Ratio  
 $+$ : Axial Tension — : Axial Compression